# Experimental and Analytical Evaluation of Composite Action between Steel Girders and Fiber-Reinforced Polymer Bridge Decks


**Chung-Che Chou**
*Professor, Dept. of Civil Engineering, National Taiwan University, Taiwan, cechou@ntu.edu.tw*
*Researcher, National Center for Research on Earthquake Engineering, Taiwan.*

**Yi Chen**
*Graduate Student Researcher, Dept. of Civil Engineering, National Taiwan University, Taiwan.*

**SUMMARY**
Push-off tests were conducted on six specimens to investigate the connection behavior between a steel girder and a fiber-reinforced polymer (FRP) composite bridge deck. The FRP deck panel was grouted to steel girders using shear studs, which were welded on the top of the girder corresponding to every alternate cell of the deck. Test parameters included type of decks, number of studs, and diameter of studs. Specimens during push-off tests exhibited about 10-mm slip before failure; failure modes were fracture of shear studs, leading to separation between the deck and girder. The ultimate shear strength of the FRP deck-to-girder connection was overestimated per AASHTO-LRFD bridge design specifications (2004) due to gout crack opening and bedding layer damage. A general-purpose nonlinear finite element analysis program was also used to perform a correlation study. Based on experimental and analytical results, design recommendations for the FRP deck-to-girder connection was proposed.

*Keywords: Composite action, Shear stud, Fiber-reinforced polymer deck, Push-off test, Finite element analysis*

## 1. INTRODUCTION

The fiber-reinforced polymer (FRP) deck can be incorporated in the new construction of bridges since it does not require framework in place, and it can save construction time as well. However, FRP composites cost more initially than conventional materials used in bridges. To save the construction cost, researchers have attempted to investigate combinations of the FRP deck and conventional materials such as steel, concrete, or FRP girders. Seible et al. (1998), Davol (1998), and Zhao (1999) investigated a two span bridge with light weight concrete filled in circular FRP composite tubes with a pultruded FRP deck. One of the challenges with the FRP deck was to develop a reliable connection between the FRP deck and concrete-filled FRP tubes. The deck-to-girder shear connection used steel dowels, which were grouted in the core of a circular FRP girder by lightweight concrete.

A very limited number of FRP bridges are constructed compositely with steel girders. Zhou et al. (2005) investigated FRP deck-to-steel girder connections, which used A325 bolts or J-bolts to fasten the deck and girder flange. The connection designs were not intended to develop composite action between the deck and girders. However, the lack of composite action causes a slip between the bottom face of the FRP deck and the top face of the girder when the bridge is loaded. Therefore, full composite action is desired to prevent a slip. Moon et al. (2002) investigated the composite action between steel girders and the Martin Marietta Composites (MMC) Gen4 FRP deck using shear studs for the Ohio Department of Transportation Bridge. Tests indicated local crushing or delamination of the FRP deck, which consists of pultruded elements bonded together to form a trapezoidal-core sandwich structure. Due to the discrete nature of FRP decks, the maximum shear strength was 60–70% of the capacity obtained by shear stud connections tested by Ollgaard et al. (1971) for concrete decks. Alnahhal et al. (2008) conducted flexural loading tests for a FRP deck on steel girders. The FRP deck, which comprises trapezoidal cell units surrounded by an outer shell, was connected to steel girders using 13-mm diameter shear studs. Experimental results indicated that the FRP deck provided partial composite action with steel girders during the test. Vyas et al. (2009) also conducted flexural loading tests for a FRP deck on steel girders by using studs for shear transfer. The FRP deck, which differs from the trapezoidal cell deck, consists of a top flat panel and bottom panel that includes four T

sections and a flat bottom plate pultruded as one piece. Proof tests of two-span specimens with steel girders and the FRP deck exhibited no damage in the FRP deck and deck-to-girder connections. However, the maximum shear strength, failure mode, and debonding mechanism between the FRP deck with T sections and steel girders remain unclear.

This study investigated the composite action between the FRP deck with T sections and steel girders. The paper begins by introducing the test program conducted at the National Center for Research on Earthquake Engineering (NCREE), Taiwan. The previous research on deck-to-steel girder connections is then presented. Next, test results are summarized along with an outline of damage progression and failure modes observed in each test. Those results are then compared with those of previous studies. Furthermore, finite element analysis is conducted on specimens to perform a correlation study in order to examine the effects of shear studs on the FRP deck-to-girder performance and sources of failure. Based on experimental and finite element analysis results, recommendations are made on how to design FRP deck-to-steel girder connections.

## 2. DESCRIPTION OF THE FRP DECK AND STEEL GIRDER ASSEMBLY

The deck consists of mechanically fastened pultruded glass FRP parts. A bottom panel that includes four T sections and a flat bottom plate is pultruded as one piece (Fig. 1(a)). A pultruded top plate is then placed and mechanically fastened to the top flanges of the bottom panel. The direction of the T section is placed transversely to the longitudinal direction of steel girders (Fig. 1(b)). The FRP deck and steel girders are connected using shear studs and grout.

Shear stud strength in concrete is normally evaluated by push-off tests. Previous studies of Ollgaard et al. (1971) showed that the ultimate strength of shear studs depends on the concrete compressive strength, elastic modulus, shank area and tensile strength of the stud:

$$P_u = 0.5 A_{sc} \sqrt{f'_c E_c} \le A_{sc} F_u \tag{1}$$

$$E_c = w^{1.5} 0.0428 \sqrt{f'_c} \tag{2}$$

where $P_u$ is the nominal shear capacity of one stud (N), $A_{sc}$ is the area of a shear stud (mm$^2$), $f'_c$ is the compressive strength of concrete (MPa), $E_c$ is the elastic modulus of concrete (MPa), and $F_u$ is the ultimate tensile strength of a shear stud (MPa). Eqs. (1) and (2) are adopted in AASHTO-LRFD (2004) and EUROCODE-4 (1997) for only concrete deck, not FRP deck to steel girders.

A bedding layer as shown between the FRP deck and steel girder (Fig. 1(b)) is inevitable since the FRP deck is placed on steel girders, in which change of the girder section, connection details, and elevation adjustment are considered. The bedding layer thickness is determined by the configuration of bridges. The bedding layer is thin without reinforcement and easily cracked at a relatively low load. Therefore, Shim et al. (2001) developed an empirical equation by considering the effect of the bedding layer on the ultimate strength of the shear connection:

$$P_u = \alpha(0.36 A_{sc} + 18.714) \tag{3}$$

$$\alpha = 1 - 0.0086(B_h - 20) \tag{4}$$

where $\alpha$ is the reduction factor considering the bedding layer, and $B_h$ is the bedding layer thickness (mm). Moon et al. (2002) conducted tests for determining a practical connection, capable of developing composite actions between steel girders and the Martin Marietta Composites Gen4 FRP deck. Bearing strength of the bottom face sheet represented a lower bound, and shear stud capacity represented an upper bound of shear strength of the connection. Shear stud connections without spirals failed due to premature loss of grout confinement, followed by local crushing of the composite deck. Therefore, Eq. (1) was modified to include this new failure mode of the FRP deck:

$$P_u = t_{fs} d_s F_c \le A_{sc} F_u \tag{5}$$

where $t_{fs}$ is the thickness of bottom face sheet (mm), $d_s$ is the diameter of a shear stud (mm), and $F_c$ is the bearing strength of FRP material (MPa). However, a hole in the FRP deck is normally larger than the stud diameter, so the strength of the FRP deck bearing against grout is modified in this study:

$$P_u = t_{fs} w_{fs} F_c \le A_{sc} F_u \tag{6}$$

where $w_{fs}$ is the hole width in the FRP deck.

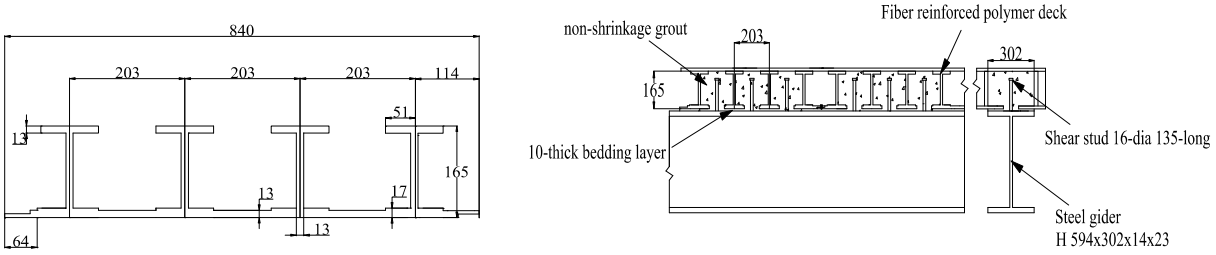


(a) FRP Deck Cross Section (Bottom Panel) (b) FRP Deck Connected to Steel Girder

**Figure 1.** FRP deck (unit: mm)

## 3. TEST SPECIMENS

Six deck-to-steel girder specimens were designed and tested to investigate the behavior of shear studs in the FRP deck. Parameters considered in these specimens were deck types, diameter of studs, and number of studs (Table 1). Specimens 1 and 2 had a deck, which consisted of #3 reinforcement and non-shrinkable grout. Specimens 1 and 2 had two shear studs per row with a spacing of 100 mm, and one deck was grouted to a steel girder by six studs (Fig. 2(a)). Diameters of shear studs in Specimens 1 and 2 were 16 and 22 mm, respectively. Four specimens used the FRP deck, which was fabricated by the Zellcomp Inc., United States. The FRP deck panels were grouted to a steel girder using shear studs, which were welded on top of the girders at locations corresponding to every alternate cell of the FRP deck (Fig. 2(b) and 2(c)). Specimen 3 had two 16-mm diameter studs per cell, while Specimen 4 had one 16-mm diameter stud per cell. Specimen 5 had two 22-mm diameter studs per cell, while Specimen 6 had one 22-mm diameter stud per cell. Shear studs used in this study were 150 mm in length, and had a minimum specified yield strength of 480 MPa. The steel girder section was 594×302×14×23 (mm), specified to be ASTM A572 Gr. 50. Holes with four times the stud diameter were drilled on the bottom of the pultruded deck panels to match the pattern of studs. The deck panels were placed on the girders by inserting studs through holes. Grout was poured with a mixture of a specified strength of 60 MPa for all specimens on the same day; in addition, 18 cubic cylinders were made for the material test.

Tables 2 and 3 list the material strengths for the steel girder, shear stud, and grout on the day of testing. Since the bearing strength of the FRP bottom deck (Eq. (6)) and grout strength (Eq. (1)) exceeded the stud strength ($A_{sc}F_u$), shear failure of studs was expected in all specimens. Each stud tensile capacity, as calculated by Eq. (1) of the AASHTO-LRFD bridge design specifications (2004), was 117 kN for the 16-mm diameter stud and 190 kN for the 22-mm diameter stud. The ultimate shear strength based on Eq. (3), which considers the effect of the bedding layer on the reduction of grout strength, was about 10-15% lower than that based on Eq. (1). However, local damage of the FRP deck calculated based on Eq. (5) was the lowest among other predictions, indicating a potential failure of the FRP bottom deck.

**Table 1.** Specimen design parameters

| Specimen | Stud Number | Stud Diameter (mm) | Deck |
|---|---|---|---|
| 1 | 12 | 16 | Grout |
| 2 | 12 | 22 | Grout |
| 3 | 12 | 16 | FRP |
| 4 | 6 | 16 | FRP |
| 5 | 12 | 22 | FRP |
| 6 | 6 | 22 | FRP |

**Table 2.** Material strengths of steel girder and stud

| Item | Yield Strength (MPa) | Ultimate Strength (MPa) |
|---|---|---|
| Beam Flange | 390 | 528 |
| Beam Web | 406 | 540 |
| Stud (Dia.=22mm) | 480 | 500 |
| Stud (Dia.=16mm) | 480 | 580 |

**Table 3.** Grout strength on day of test

| Specimen | Cubic 1 (MPa) | Cubic 2 (MPa) | Cubic 3 (MPa) | Average (MPa) |
|---|---|---|---|---|
| 1 | 62 | 60 | 64 | 62 |
| 2 | 68 | 69 | 69 | 69 |
| 3 | 53 | 50 | 45 | 50 |
| 4 | 61 | 59 | 59 | 61 |
| 5 | 68 | 72 | 59 | 68 |
| 6 | 59 | 58 | 62 | 61 |

(a) Specimens 1 and 2

(b) Specimen 3

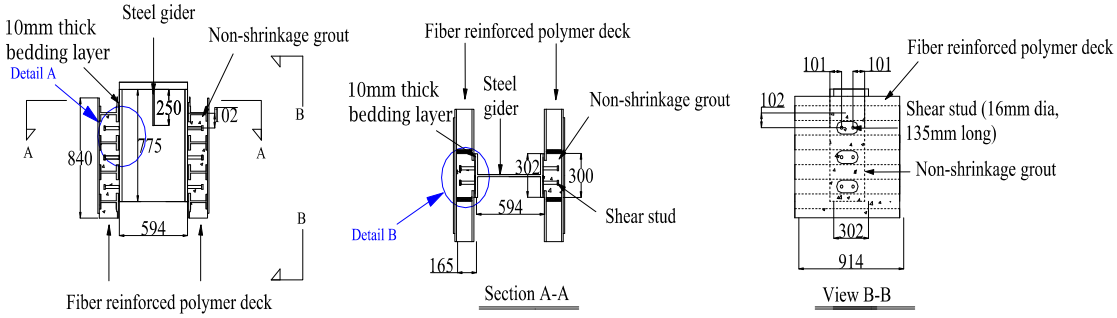


(c) Specimen 3 Details

**Figure 2.** Specimen details (unit: mm)

## 4. TEST PROGRAM AND RESULTS

Fig. 3 shows the test setup used for evaluating the static shear strength of individual specimens. Specimens were loaded at a constant rate until failure. Several linear displacement transducers were placed in the specimen to measure the relative displacement (slip) between the girder and FRP deck. Table 4 summarizes the test results, force per stud, and corresponding slippage, where $F_{max}$ is the ultimate actuator force recorded from the load cell, $P_u$ is the ultimate shear strength per stud, $P_y$ is the yield shear strength per stud, and $\Delta_u$ and $\Delta_y$ are the corresponding slip at the ultimate shear strength and yield strength levels, respectively. Table 4 also lists the ratio between the stud capacity obtained from the test and that given by the AASHTO LRFD bridge design specifications (2004). The same failure mode was observed in all specimens, in which stud failure occurred by shear at the top of welds. Damage resulting from fiber failure or delamination in the FRP deck was not observed in Specimens 3-6. All specimens did not fail suddenly, but instead, once the ultimate shear strength was achieved, excessive damage to shear studs decreased the magnitude of load to lower values.

### 4.1 Observed Performance

For Specimens 1 and 2, shear studs were embedded in the grout deck with no bedding layers. Minor cracks were observed in the deck surface, and shear studs fractured at the end of test, leading to separation between the grout deck and steel girder (Fig. 4(a)).

For Specimens 3-6 with the FRP deck, test results indicated two important characteristics of the shear connection in the grout cell. Splitting cracks occurred in the bedding layer near the yield load level, and the bedding layer then fell apart with an increasing slip (Fig. 4(b)). At around 5-mm slip, cracks occurred in the FRP grout cell, widening and propagating with a slip (Fig. 4(c)). All specimens with the FRP deck failed due to fractures of shear studs (Fig. 4(d)) and experienced separation between the steel girder and FRP deck. The flexural deformation at the base of studs near the welds was large because the bearing grout behind the studs was lost. The load increase in specimens with the FRP deck was not obvious after passing yield strength (Fig. 5), which differed from those observed in specimens with the grout deck.

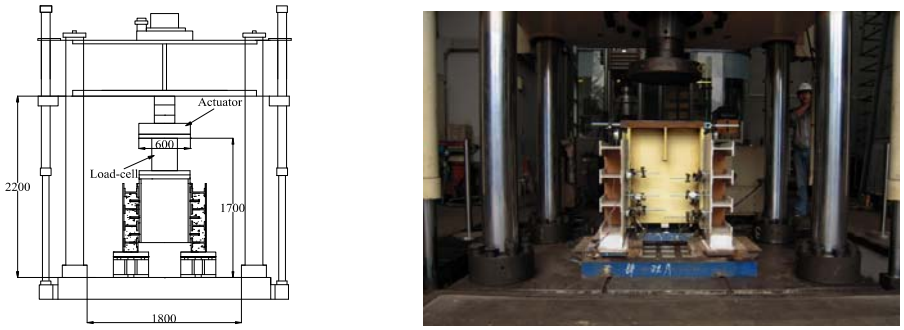


**Figure 3.** Test setup (unit: mm)

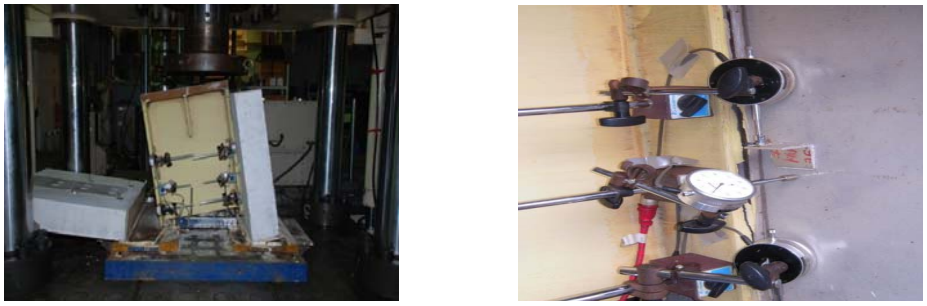

(a) Specimen 1 (b) Specimen 5 (Bedding Layer Splitting)

(c) Specimen 5 (Grout Cracking) (d) Shear Stud Fracture

**Figure 4.** Observed performance in Specimens under push-off tests

**Table 4.** Strength and deformation of shear studs in tests

| Specimen | $F_{max}$ (kN) | $P_u$ (kN) | $P_y$ (kN) | $\Delta_u$ (mm) | $\Delta_y$ (mm) | $\frac{P_u}{A_{sc}F_u}$ | Failure Mode |
|---|---|---|---|---|---|---|---|
| 1 | 1782 | 149 | 82 | 7.8 | 0.7 | 1.27 | Stud Fracture |
| 2 | 2695 | 225 | 140 | 9.6 | 1.2 | 1.18 | Stud Fracture |
| 3 | 1265 | 105 | 80 | 7.3 | 0.5 | 0.90 | Stud Fracture |
| 4 | 529 | 88 | 77 | 8.6 | 0.6 | 0.75 | Stud Fracture |
| 5 | 2127 | 177 | 142 | 12 | 1 | 0.93 | Stud Fracture |
| 6 | 1055 | 176 | 140 | 12.5 | 0.6 | 0.93 | Stud Fracture |

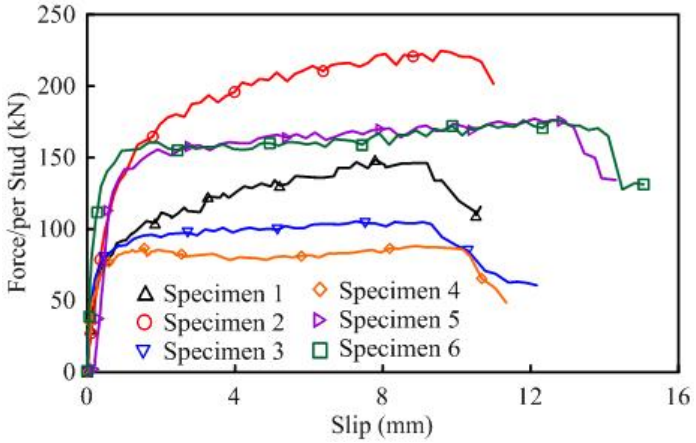


**Figure 5.** Load versus slip relationship for all specimens

### 4.2 Type of Decks

Specimens 1 and 3 had two 16-mm diameter studs per row, and Specimens 2 and 5 had two 22-mm diameter studs per row. The difference between Specimens 1 and 3, as well as that between Specimens 2 and 5 was the deck type. Fig. 5 shows the typical load/per stud versus slip relationship. Each shear connection exhibited substantial inelastic deformations prior to failure. Although different decks were used in Specimens 1 and 3, both specimens showed a similar yield strength of 80 kN/per stud, but with different post-yield behaviors. After the yield strength was reached, the load in Specimen 1 with the grout deck increased with slip; however, that of Specimen 3 with the FRP deck exhibited a large yield plateau until failure. A similar response was observed in Specimens 2 and 5 using 22-mm diameter shear studs, all of which had a yield strength of around 140 kN/per stud. The load increase was apparent in Specimen 2 with the grout deck, yet not obvious in Specimen 5 with the FRP deck.

### 4.3 Number of Studs

Specimens 3 and 4 differed in the number of studs per grout cell. Specimens 3 and 4 used two 16-mm diameter studs and one 16-mm diameter stud per grout cell, respectively. Both specimens were similar in the yield strength per stud (Fig. 5), but the ultimate strength per stud differed by 15%. Specimens 5 and 6 also differed in the number of studs per grout cell. Specimens 5 and 6 used two 22-mm diameter studs and one 22-mm diameter stud per grout cell, respectively. Both specimens were also similar in the yield strength per stud, and both specimens differed by 1% in terms of the ultimate strengths per stud. Therefore, one stud or two studs placed 10 cm away in a grout cell of the FRP deck achieved a similar load capacity. Compared to the grout deck, damage in the bedding layer and grout cell decreased ultimate strength of shear studs in the FRP deck. Table 4 shows that, except for Specimen 4, the ultimate strength of a shear stud used in the FRP deck is about 90% of the tensile strength calculated by Eq. (1) and is close to that predicted by considering the effect of the bedding layer on strength reduction (Eq. (5)).

## 5. FINITE ELEMENT ANALYSIS

An analytical study was conducted for six specimens under push-off tests. By using the finite element analysis program ABAQUS (2009), this study developed finite element models of specimens that can examine the structural responses and sources of stud fracture. Fig. 6 shows an analytical model comprising a steel girder, deck, and shear studs. Yield and ultimate stresses obtained from coupon tests were adopted for each specimen (Table 2). Material nonlinearity with the von Mises yielding criterion was considered in the girder and shear studs. Since the FRP deck was not damaged during the test, the FRP deck considered only elastic behavior. Additionally, nonlinear behavior of the grout under compression was modeled using the Damaged Plastic function in the computer program. Eight-node solid elements, C3D8R, with three degrees of freedom at each node were used in the steel

beam, grout, and shear studs. Four-node shell elements, S4R, were used for the FRP deck. An interaction element between the grout and studs, FRP deck, and steel flange was modeled with a hard contact behavior, allowing for separation of the interface in tension and no penetration of that in compression. The interaction element has been successfully used to prevent penetration of a steel core to a restraining member of the buckling-restrained brace under compression (Chou and Chen 2009, 2010) and gap opening/closing behavior of steel dual-core self-centering braces under seismic loading (Chou et al. 2006, Chou and Chen 2012). Axial displacement was applied at the top of the steel girder to simulate load transfer during the test.

Fig. 7 shows the load versus slip relationship in all specimens. For Specimens 1 and 2 with the grout deck, the ultimate shear strength obtained from the finite element analysis correlates well with the test results. For Specimens 3-6 with the FRP deck, although the yield shear strengths obtained from finite element analyses also correlates well with the test results, the ultimate shear strengths in models increases within the post-yield range, which does not exhibit the yield plateau, as observed in the tests. This behavior is caused by splitting in the bedding layer and crack opening in the grout cell, which are not simulated in the models. Except for Specimen 4, the error in predicting the ultimate shear strength ranges from 4-15%. The plastic equivalent strain (PEEQ) was computed at locations near stud welds to identify possible sources of fracture. It shows that the shear strain is much larger than the tensile strain in studs, which significantly contributes to PEEQ and rupture of shear studs.

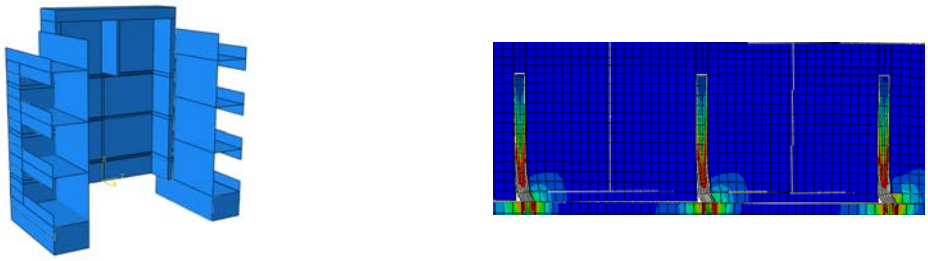

**Figure 6.** Finite element model (Specimen 4)

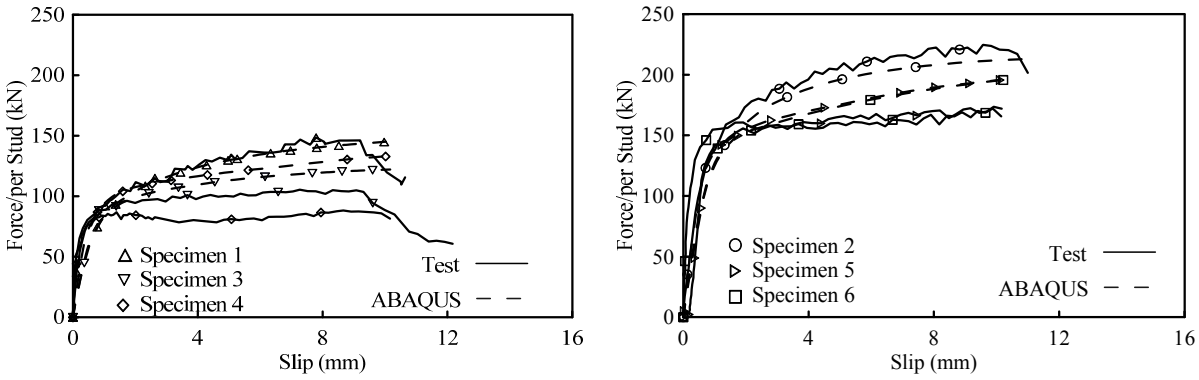


(a) Specimens 1, 3 and 4 (b) Specimens 2, 5 and 6

**Figure 7.** Comparison between test and finite element analysis

## 6. CONCLUSIONS

This study investigates experimentally and analytically the composite action between the FRP deck and steel girder. Shear studs with non-shrinkage grout connect the FRP deck and steel girder. Two specimens were made using the grout deck, and four specimens were made using the FRP deck. Parameters in the specimens were the type of decks, number of studs, and diameter of studs. Push-off test and finite element analysis results of the deck-to-steel girder connections are summarized as follows:

1. Fracture of studs was only the failure mode in all specimens. No visible sign of damage or delamination was observed in the FRP deck, indicating that a hole width equal to four times stud

diameter can be used in design. Full composite action was achieved before yield strength of studs, which was observed in either the grout deck or FRP deck specimens. Ultimate strength of shear studs in the grout deck exceeded the design strength, which is specified by the AASHTO-LRFD bridge design specifications (2004). Except for Specimen 4, the ultimate strength of shear studs in the FRP deck was about 10% lower than that specified by the AASHTO-LRFD bridge design specifications (2004) due to damage in the bedding layer and grout cell.

2. Comparing ultimate shear strengths obtained in the FRP-deck specimens, 22-mm diameter studs in Specimens 5 and 6 achieved a load capacity 1.7 to 2 times that of 16-mm diameter studs in Specimens 3 and 4. The load increasing ratio was close to the cross-sectional area ratio (1.9) of the 22-mm diameter stud to the 16-mm diameter stud. Moreover, two studs in a grout cell placed 100 mm away achieved load capacity twice that of one stud in a grout cell.
3. The finite element models can estimate the load versus slip relationship of Specimens 1 and 2 with the grout deck, but not for Specimens 3-6 with the FRP deck. This is owing to modeling inability for grout crack opening and bedding layer splitting. Furthermore, shear studs experience a significantly larger shear strain than tensile strain at failure, causing fracture of studs in all specimens.

## ACKNOWLEDGMENTS

The authors would like to thank the National Center for Research on Earthquake Engineering (NCREE), Taiwan for financially supporting the project. The authors would also like to thank Dr. Dan Richards, President of ZellComp Inc. Unite States, and Meg Richards for providing valuable advices to the test program.

## REFERENCES

Alnahhal W., Aref A., Alampalli S. (2008). Composite behavior of hybrid FRP-concrete bridge decks on steel girders. Composite Structures. 84. 29-43.

Chou C-C, Chen J-H, Chen Y-C, and Tsai K-C. (2006). Evaluating performance of post-tensioned steel connections with strands and reduced flange plates. *Earthquake Engineering and Structural Dynamics*, 35(9), pp. 1167-1185.

Chou C-C, Chen P-J. (2009). Compressive behavior of central gusset plate connections for a buckling-restrained braced frame. *J. Constructional Steel Research*, 65(5), 1138-1148.

Chou C-C, Chen S-Y. (2010). Subassemblage tests and finite element analyses of sandwiched buckling-restrained braces. *Engineering Structures*, 32, 2108-2121.

Chou C-C, Chen Y-C. (2012). Development and seismic performance of steel dual-core self-centering braces. *15th World Conference on Earthquake Engineering*, Lisboa, Portugal.

Davol A. (1998). Structural Characterization of Concrete Filled Fiber Reinforced Shells. *Ph.D. dissertation*, University of California, San Diego, CA.

Eurocode-4. (1997). Design of composite steel and concrete structures, Part 2: Composite bridges. CEN.

HKS (2009). ABAQUS User's Manual Version 6.9, Hibbitt, Karlsson & Sorensen, Pawtucket, RI.

LRFD Bridge Design Specifications. (2004). 3rd Ed., American Association of State Highway and Transportation Officials (AASHTO), Washington, D.C.

Moon FL, Eckel DA, Gillespie JW. (2002). Shear stud connection for the development of composite action between steel girders and fiber reinforced polymer bridge decks. *J. Struct. Engrg.* ASCE;128(6): 762–770.

Ollgaard JJ, Slutter RG, and Fisher JW. (1971). Shear strength of stud connectors in lightweight and normal-weight concrete. *Eng. J.*, 55–64.

Shim CS, Chang SP, Lee PG. (2001). Design of shear connection in composite steel and concrete bridges with precast decks. *J. Constructional Steel Research*, 2001; 57: 203–219.

Seible F, Karbhari VM, Burguen˜o R, Seaberg E. (1998). Modular advanced composite bridge systems for short and medium span bridges. Developments in short and medium span bridge engineering. *Proceedings of the 5th international conference on short and medium span bridges*. Canadian Society of Civil Engineers: Calgary (Canada), 431–441.

Vyas JS, Zhao L, Ansley MH, Xia J. (2009). Characterization of a low-profile fiber-reinforced polymer deck system for moveable bridges. *J. Bridge Engrg.*, ASCE;14(1); 55-65.

Zhao L. (1999). Characterization of deck-to-girder connections in FRP composite superstructures. *Ph. D. dissertation*, University of California, San Diego, CA.

Zhou A, Coleman JT, Temeles AB, Lesko JJ, and Cousins TE. (2005). Laboratory and field performance of cellular fiber-reinforced polymer composite bridge deck systems. *J. Composites for Construction*, 9(5), 458-467.